Trafficking of ODV-E66 is mediated via a sorting motif and other viral proteins: Facilitated trafficking to the inner nuclear membrane

Sharon C. Braunagel*, Shawn T. Williamson†, Suraj Saksena‡, Zhenping Zhong*, William K. Russell§, David H. Russell§, and Max D. Summers*†‡¶‖

Departments of †Biology, ‡Biochemistry and Biophysics, §Chemistry, and ¶Entomology and *Texas Agricultural Experiment Station, Texas A&M University, College Station, TX 77843-2475

Contributed by Max D. Summers, April 20, 2004

The N-terminal 33 aa of the envelope protein ODV-E66 are sufficient to traffic fusion proteins to intranuclear membranes and the ODV envelope during infection with *Autographa californica* nucleopolyhedrovirus. This sequence has two distinct features: (*i*) an extremely hydrophobic sequence of 18 aa and (*ii*) positively charged amino acids close to the C-terminal end of the hydrophobic sequence. In the absence of infection, this sequence is sufficient to promote protein accumulation at the inner nuclear membrane. Covalent cross-linking results show that the lysines of the motif are proximal to FP25K and/or BV/ODV-E26 during transit from the endoplasmic reticulum to the nuclear envelope. We propose that the 33 aa comprise a signature for sorting proteins to the inner nuclear membrane (sorting motif) and that, unlike other resident proteins of the inner nuclear membrane, ODV-E66 and sorting-motif fusions do not randomly diffuse from their site of insertion at the endoplasmic reticulum to the nuclear envelope and viral-induced intranuclear membranes. Rather, during infection, trafficking is mediated by protein–protein interactions.

Baculovirus infection provides an amplified pulse of integral membrane proteins that use the continuous membranes of the endoplasmic reticulum (ER), outer nuclear membrane (ONM), nuclear pore membrane, and inner nuclear membrane (INM) during their transit to the viral envelope of the occlusion-derived virus (ODV). In 1997, Hong *et al*. (1) showed that the N-terminal region of the envelope protein ODV-E66 (E66) was sufficient to traffic fusion proteins to intranuclear membranes and the ODV envelope during infection with *Autographa californica* nucleopolyhedrovirus. This sequence has two distinct features: (*i*) an extremely hydrophobic sequence of 18 aa and (*ii*) positively charged amino acids close to the C-terminal end of the hydrophobic sequence. We propose that these characteristics comprise a signature for sorting proteins to the INM that we now refer to as an INM-sorting motif (SM).

When ODV envelope proteins are expressed under their native promoters, they locate so rapidly to viral-induced intranuclear microvesicles and the ODV envelope that intermediates in the trafficking pathway are difficult to discern. When large quantities of E66 or SM fusions are expressed by using recombinant viruses, the proteins are easily detected in the ER, ONM, and INM, suggesting that the proteins use these continuous membranes during trafficking. Because other observable viral phenomena (e.g., microvesicle formation, viral maturation, etc.) are similar to wild type, it is likely that these viral proteins are simply more abundant in their normal pathway (1).

In this study we used a series of SM-fusion proteins to study trafficking of viral proteins from their site of insertion at the ER to the nuclear envelope. Even in the absence of infection, this sequence is sufficient to direct proteins to the INM. During infection, SM-fusion protein trafficking to the nuclear envelope is facilitated by other viral proteins: FP25K and/or BV/ODV-E26 (E26).

Materials and Methods

Insect Cell Lines and Virus. *Spodoptera frugiperda* (Sf9) cells were cultured as described (2). Nucleopolyhedrovirus-E2 strain was used at a multiplicity of infection of 20.

***In Vitro* Glycosylation Assay.** Dog pancreatic or infected Sf9 cell microsomes (33 h after infection), signal-recognition particle, and wheat germ extract were prepared (3, 4). PCR and *in vitro* transcription were used to generate mRNA containing an *N*-GlcNAc acceptor sequence (Fig. 1*A*, constructs 2 and 4). The mRNA was translated by using wheat germ extract in the presence of 40 nM canine signal-recognition particle, [^{35}S]Met (0.2 μCi/μl; 1 Ci = 37 GBq), and microsomal membranes. Attached ribosomes were removed by using 2 mM puromycin (26°C for 10 min). After translation, samples were treated with endoglycosidase H or peptide *N*-glycosidase as described by Braunagel *et al*. (5). Membranes were sedimented through a sucrose cushion and analyzed by using SDS/PAGE.

Sf9 Cell Transfection, Selective Permeabilization, and Confocal Microscopy. Sf9 cells were transfected by using calcium phosphate (2). Digitonin permeabilization was performed essentially as described by Adam *et al*. (6). Cells were fixed with 3.7% paraformaldehyde (room temperature, 10 min), washed three times, and incubated either with digitonin (30 μg/ml: semipermeabilization) or as described by Rosas-Acosta *et al*. (7) (full permeabilization). Slides were viewed by using a Zeiss Axiovert 135 microscope with a CARV confocal module (Zeiss Micro-Imaging and Atto Bioscience) and images were collected at 0.75-μm intervals. After viewing at least 20 fields, representative cells were collected by using Zeiss AXIOVISION 3.1. Antibodies used were ADL67-*Drosophila* lamin [1:250 (8)], calnexin-CT (1:500; StressGen Biotechnologies, Victoria, Canada), calreticulin (1:1,000; Affinity BioReagents, Golden, CO), and GFP (1:1,000; Chemicon International).

Immunoprecipitation, SDS/PAGE, and Western Blot. Used for each precipitation were 1.5×10^6 cells. At the appropriate time, cells were collected and resuspended in 500 μl of lysis buffer (50 mM Tris, pH 8.0/150 mM NaCl/0.1% SDS/0.5% sodium desoxycholate/0.5% Triton X-100). The cell extract was preabsorbed with 20 μl of preimmune serum followed by 20 μl of protein A/G agarose (50% slurry; Sigma) for 1 h at 4°C. The preadsorbed extract was precipitated by using 10 μl of antibody overnight followed by a 2-h incubation with 20 μl of protein A/G agarose.

Abbreviations: ER, endoplasmic reticulum; ONM, outer nuclear membrane; INM, inner nuclear membrane; ODV, occlusion-derived virus; E66, ODV-E66; SM, sorting motif; E26, BV/ODV-E26; TM, transmembrane.

‖To whom correspondence should be addressed. E-mail: m-summers@tamu.edu.

www.pnas.org/cgi/doi/10.1073/pnas.0402727101

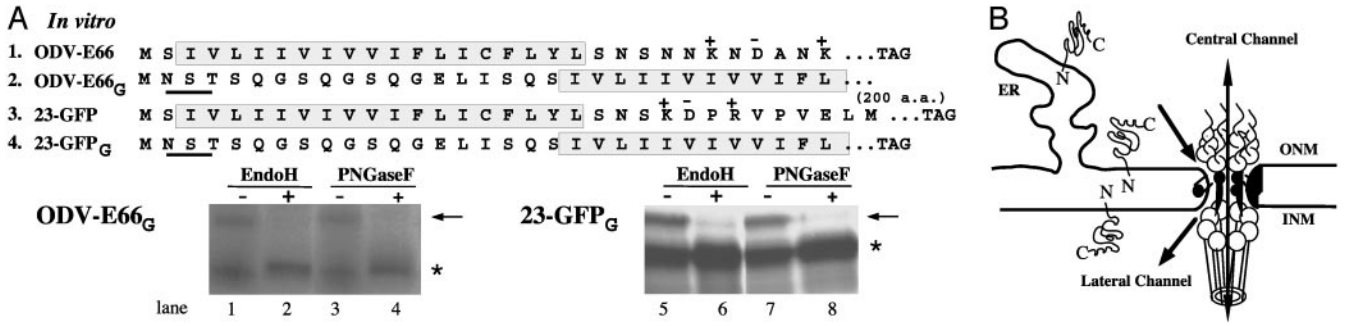

Fig. 1. Orientation of 23-GFP and E66. (*A*) Construct 1 is the native sequence E66. Construct 2 shows the added *N*-GlcNAc acceptor sequence (underlined). Constructs 3 and 4 show an equivalent sequence modification of 23-GFP. Lanes 1–4 show *in vitro* translation of $E66_G$, and lanes 5–8 show an equivalent experiment using $23\text{-}GFP_G$. −, translation in the presence of microsomal membranes; +, paired reaction with the addition of enzyme; *, unmodified protein; arrow, glycosylated protein. (*B*) Schematic orientation of protein in the ER, ONM, pore membrane, and INM.

The bound A/G agarose was washed three times in lysis buffer and analyzed by using SDS/PAGE and Western blot. Western blots were performed as described (7). Antibodies used were FP25K, no. 2804, 1:5,000; T7 (Novagen), 1:5,000; and E26, no. 7554, 1:5,000.

SM-Scanning Constructs. A series of enhanced-GFP fusions were constructed by using complementary oligonucleotides. Briefly, oligonucleotides were mixed in equimolar amounts, annealed, and ligated into the pIE1-3 vector. The clones were sequence-confirmed, and the corresponding amino acid sequences are shown in Fig. 3.

Covalent Cross-Linking. ***In vivo.*** Sf9 cells were infected with $_{polh}$SM-cassette recombinant virus (sequence shown in Fig. 4), and cells were collected 33 h after infection. Cells were washed, resuspended in buffer A (25 mM sodium phosphate/150 mM NaCl, pH 7.0) and frozen for 30 min. After thaw, the cell membrane was disrupted by Dounce homogenization, and nuclei were pelleted by centrifugation (1,500 × *g*, 3 min), washed, and resuspended in buffer A. For every reaction, 200 μg of protein was resuspended in 100 μl of buffer A including BS^3 (2.5 mM; Pierce Biotechnology) and incubated for 30 min (room temperature). The samples were analyzed directly, immunoprecipitated (200 μg of protein per precipitation), or purified by using Talon (BD BioSciences) or His·Mag (Novagen) beads per manufacturer instructions.

In vitro. *In vitro* translations of mRNA were performed in the presence of rabbit reticulocyte lysate (minus Met) RNasin, 8 eq of infected Sf9 microsomes, and [^{35}S]Met. After translation, membranes were sedimented through a sucrose cushion and resuspended in 50 μl of buffer A containing BS^3. The SM cassette and cross-linked complex were precipitated by using the appropriate antibodies, separated by using SDS/PAGE, and either Western blotted and probed with antibodies or visualized by using Bio-Rad Molecular Imager FX.

Results

E66 and SM Fusions Constitute Type 1 Signal Anchors. The N-terminal region of E66 constitutes a noncleaved signal anchor (9). Thus, orientation would determine the molecular mass passing through the lateral channel of the nuclear pore (Fig. 1*B*). Orientation was determined by constructing a clone that contained a consensus acceptor sequence for *N*-GlcNAc glycosylation at the N terminus of E66 or the SM fusion (Fig. 1*A*, constructs 2 and 4). The reaction was treated with endoglycosidase H or peptide *N*-glycosidase, and molecular mass was determined by using SDS/PAGE. The result shows that protein mass was reduced by treatment with either endoglycosidase H or peptide *N*-glycosidase (Fig. 1*A*, lanes 1–4). The orientation of 23-GFP was tested in a similar manner (Fig. 1*A*, lanes 5–8). These results were confirmed by using proteinase K digestion (data not shown). Thus, E66 is a type I signal anchor with the bulk of the protein exposed at the cytoplasmic face of the ER (Fig. 1*B*).

SM-Fusion Proteins Accumulate at the INM. By using transient expression, two SM-fusion proteins (33-GFP and 23-GFP) were monitored to determine their localization in the absence of infection (sequences shown in Fig. 3, group 1). Because equivalent data were obtained from either protein, results from both constructs are shown throughout this article. Three cellular markers were used: (*i*) the intermediate filament protein lamin, which resides largely at the nucleoplasmic face of the INM; (*ii*) calreticulin, a soluble, luminal protein of the ER; and (*iii*) calnexin, an ER integral membrane protein. The calnexin antibody recognizes the cytoplasmic region of the protein.

When 33-GFP was transiently expressed in Sf9 cells, it colocalized with the ER markers calreticulin (Fig. 2*B*) and calnexin (Fig. 2*C*) and formed a nuclear rim in close juxtaposition with the inner nuclear marker, lamin (Fig. 2*A*). To determine whether the SM fusion was capable of locating to the INM, Sf9 cells transiently expressing the SM fusion were prepared for electron microscopy and probed with antibody to GFP and gold-conjugated secondary antibody: 23-GFP is present at the ER, the ONM, and INM (Fig. 2*D*). These data indicate that in the absence of viral infection, 23-GFP locates throughout the ER and nuclear envelope. Thus, the lateral channels of the nuclear pore do not restrict movement at the pore membrane.

Semipermeabilization experiments were performed to determine whether the visible nuclear rimming of the SM fusion represents localization at the ER positioned at the nuclear periphery or protein at the INM. This technique utilizes cholesterol compositional differences to selectively permeabilize the plasma membrane vs. intracellular membranes to allow antibody penetration (6, 10). When the plasma membrane is permeabilized, leaving the ER and nuclear envelope intact, antibodies to lamin are not bound (Fig. 2*E1*). In contrast, lamin is visible when membranes are fully permeabilized (Fig. 2*F1*). In semipermeabilized cells, antibodies to GFP display a pattern similar to calnexin (Fig. 2*E2*); however, autofluorescence of 33-GFP clearly shows a nuclear rim (Fig. 2*E2*). When cells are fully permeabilized, antibodies to GFP show the same pattern as autofluorescence (Fig. 2*F*). These results show that nuclear rimming represents protein accumulation at the INM.

CELL BIOLOGY

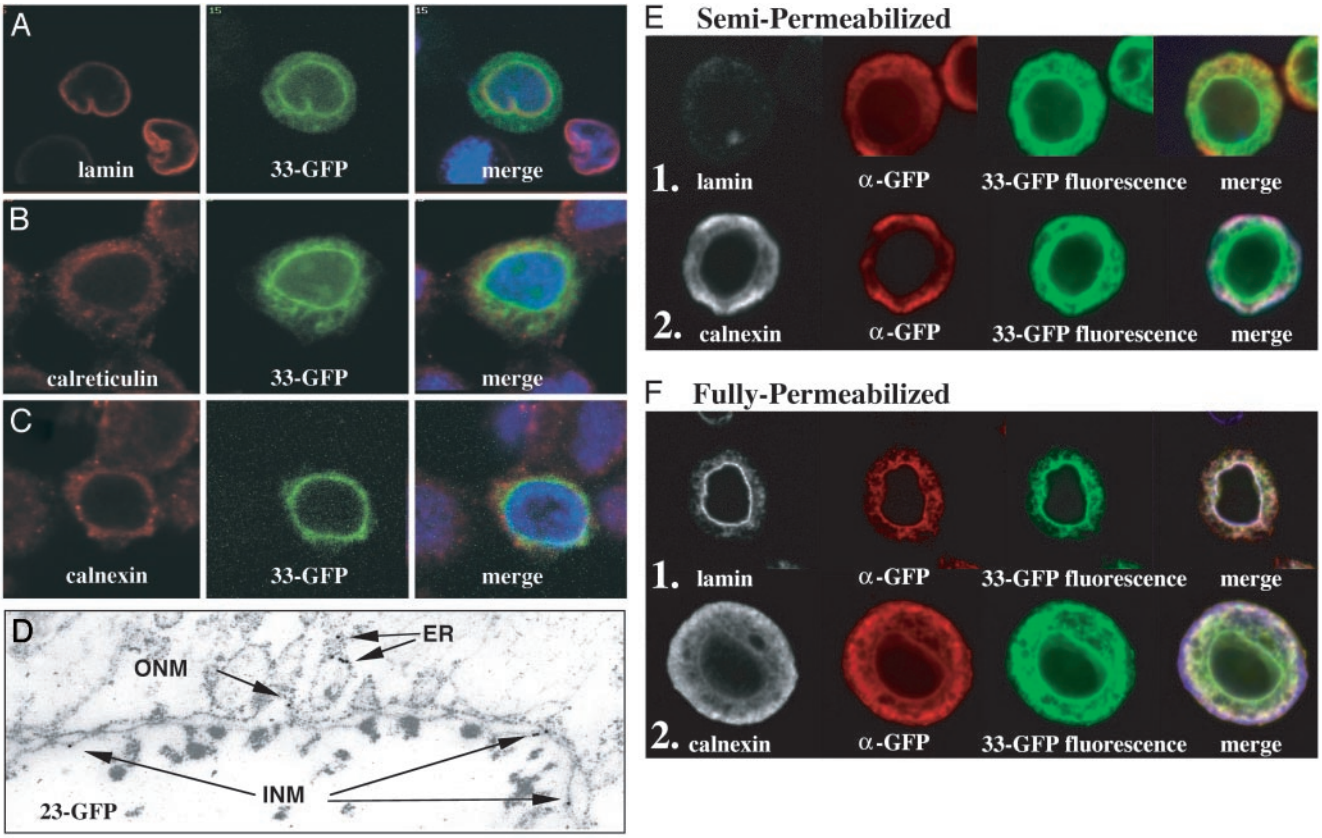

Fig. 2. Localization of SM fusion in Sf9 cells during transient expression. The SM-fusion construct 33-GFP was transiently expressed in Sf9 cells, and a representative *Z* image through the center of the nucleus is shown. Colocalization of 33-GFP with lamin (*A*), calreticulin (*B*), and calnexin (*C*) is shown. (*D*) 23-GFP was transiently expressed in Sf9 cells, fixed, and prepared for electron microscopy. The cells were probed with antibody to GFP and gold-conjugated secondary antibody; ER, ONM, and INM localization is noted. (*E* and *F*) *Z* sections showing localization of 33-GFP transiently expressed in Sf9 cells and colocalization with lamin (row 1) and calnexin (row 2) under conditions of semi- (*E*) or full (*F*) permeabilization.

The Lysine(s) of the SM Are Important for Protein Accumulation at the Nuclear Envelope. Thinking that the cysteine within the hydrophobic sequence might be important for sorting, we generated a site-directed mutation (C → A) and evaluated the effects of the mutation on protein sorting: no effects were observed. We site-directed the aromatic residues within the transmembrane (TM) (F,Y → A) and still observed normal protein localization. Finally, we altered the distance from the C terminus of the TM to the positively charged amino acids, which resulted in a dramatic and visible change in protein localization. For reference, the localization of 23-GFP is shown (Fig. 3, group 1). If the spacing was increased to 11 aa, a less intense nuclear rim was observed, and more protein was detected at the peripheral ER (Fig. 3, group 2). When the length of the hydrophobic sequence was increased and the lysines were deleted (Fig. 3, group 3), the protein was detected at the cell surface (Fig. 3) and secreted (confirmed by immunoprecipitation; data not shown). If spacing to the lysines was decreased with minimal changes to the hydrophobic sequence, the fusion protein was dispersed throughout the ER in a pattern indistinguishable from calreticulin (Fig. 3, group 4). These data suggest that the spacing from the C-terminal end of the hydrophobic sequence and/or the composition of the amino acids between them are critical for nuclear envelope localization.

The Lysines of the SM Are Proximal to the Viral Proteins FP25K and/or E26 During Trafficking to the Nuclear Envelope. The previous experiment suggests that the lysines in the SM are at or near a functionally important site that influences the trafficking of the SM fusion. Therefore, the lysines would serve as useful probes to identify the protein environment of the SM at various points in the trafficking pathway. To this end, a cassette was designed containing the following features: (*i*) the lysines of the SM are the only ones present within the encoded protein; (*ii*) it has a purification tag; and (*iii*) it has a unique epitope tag for unambiguous identification (Fig. 4*A*). Two recombinant viruses containing this fusion cassette were generated. In both cases, the SM cassette was inserted into the polyhedrin gene locus: one under the control of the *polyhedrin* promoter and the other virus under the control of the *E66* promoter. Both viruses showed similar results, and the data obtained from the polyhedrin-expressed cassette are shown.

SM-cassette-infected cell nuclei were isolated and treated with the soluble amine–amine cross-linking reagent BS^3. One predominant cross-linked product was observed at ≈32 kDa (Fig. 4*B*, lanes 1 and 2). The SM cassette and cross-linked complex were purified by using the $(His)_6$ sequence and resolved by SDS/PAGE. The 32-kDa cross-linked band was subjected to in-gel trypsin digestion and analyzed by using matrix-assisted laser desorption ionization/time of flight MS (11). Two viral proteins were identified: FP25K and E26 (5% and 8% overall coverage, respectively). We note that an additional, higher molecular mass band was detected; however, its identity was not determined.

Immunoprecipitation was performed to confirm that FP25K and/or E26 cross-linked to the SM cassette. Antibodies to FP25K or E26 each precipitated the cross-linked protein com-

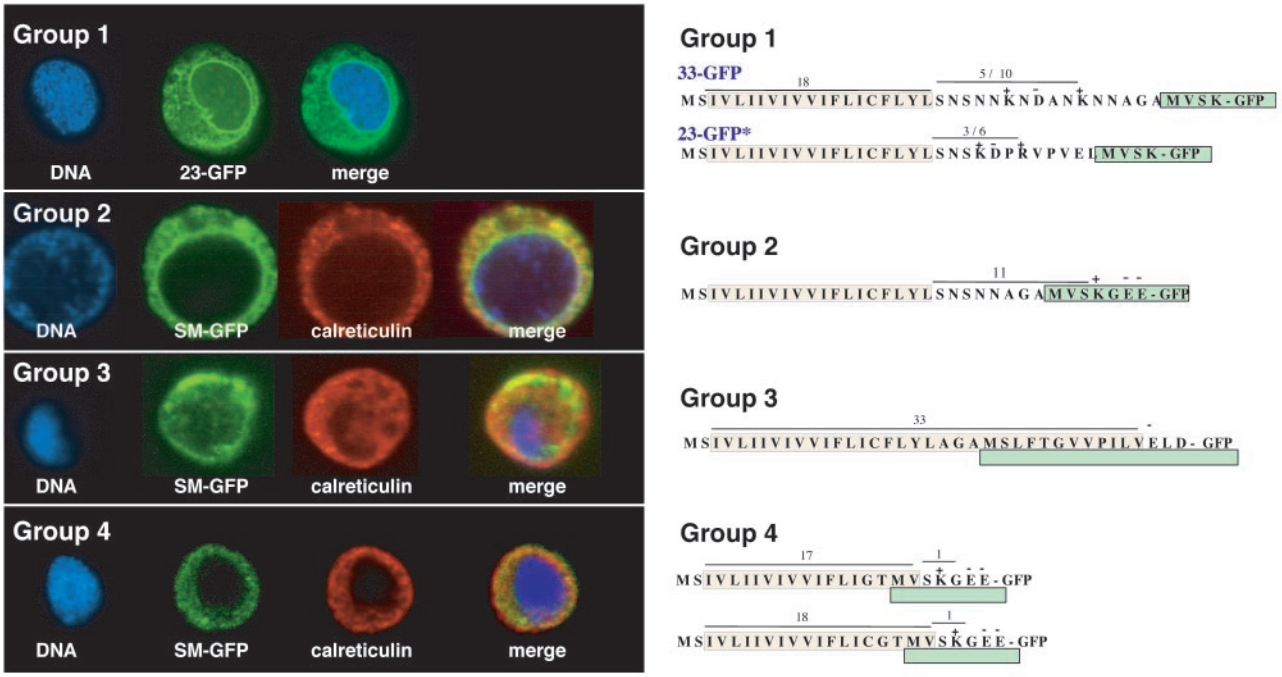

Fig. 3. Localization of SM mutants. Clones from each group were transiently expressed in Sf9 cells, and a representative *Z* section is shown. ER was identified by using antibody to calreticulin and DNA labeled with 4′,6-diamidino-2-phenylindole, whereas the SM fusion was detected by GFP autofluorescence. If two clones are represented within the same group, the results were visually indistinguishable.

plex (Fig. 4*B*, lanes 3 and 5), whereas they failed to precipitate the cassette or a protein at the molecular weight of the cross-linked complex from the negative control (Fig. 4*B*, lanes 4 and 6). The blots were reprobed with antibody to FP25K or E26, and in each case, in addition to IgGs, one band was detected: that of the free, nonbound protein (data not shown). For additional confirmation, the SM cassette and cross-linked complex were purified, separated by using SDS/PAGE, and Western blotted. T7 antibody detects both the SM cassette and cross-linked product (Fig. 4*B*, lane 10), whereas α-FP25K detected the cross-linked complex and free FP25K (Fig. 4*B*, lane 9). We note that after exposure to cross-linking reagent, antibodies to FP25K

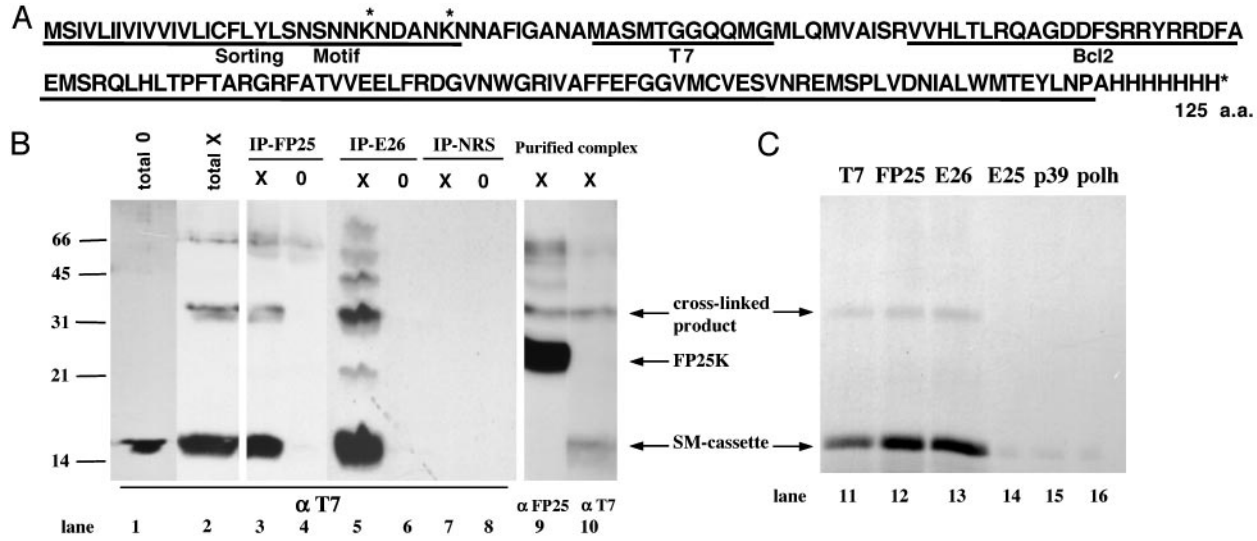

Fig. 4. The SM sequence is proximal to FP25K and E26. (*A*) Sequence of the SM cassette. Placement of the unique lysines (*), position of the T7 epitope tag, and C-terminal $(His)_6$ are shown. (*B*) Sf9 cells were infected with the $_{polh}$SM-cassette virus, cells were collected at 33 h after infection, and nuclei were purified and exposed to BS^3. 0, No cross-linker; X, addition of cross-linking reagent. The SM cassette and cross-linked adduct were detected by using antibody to T7 (lanes 1–8). Lanes 1 and 2 show total nuclear extract, whereas lanes 3–8 show product precipitated with antibodies: FP25K (lanes 3 and 4), E26 (lanes 5 and 6), and normal rabbit serum (lanes 7 and 8). Disrupted nuclear extracts were treated with Talon beads to purify the SM cassette and cross-linked complex, and proteins were separated by using SDS/PAGE and Western blotted. The identity of the proteins was determined by using antibodies to FP25K (lane 9) or T7 epitope (lane 10). (*C*) The SM cassette was translated in the presence of infected Sf9 cell microsomes (33 h after infection) and $[^{35}S]$Met, and then treated with BS^3. The proteins were precipitated by using antibodies to T7, FP25K, E26, ODV-E25, p39, and polyhedrin (lanes 11–16, respectively) and separated by SDS/PAGE, and protein was detected by using incorporated $[^{35}S]$Met.

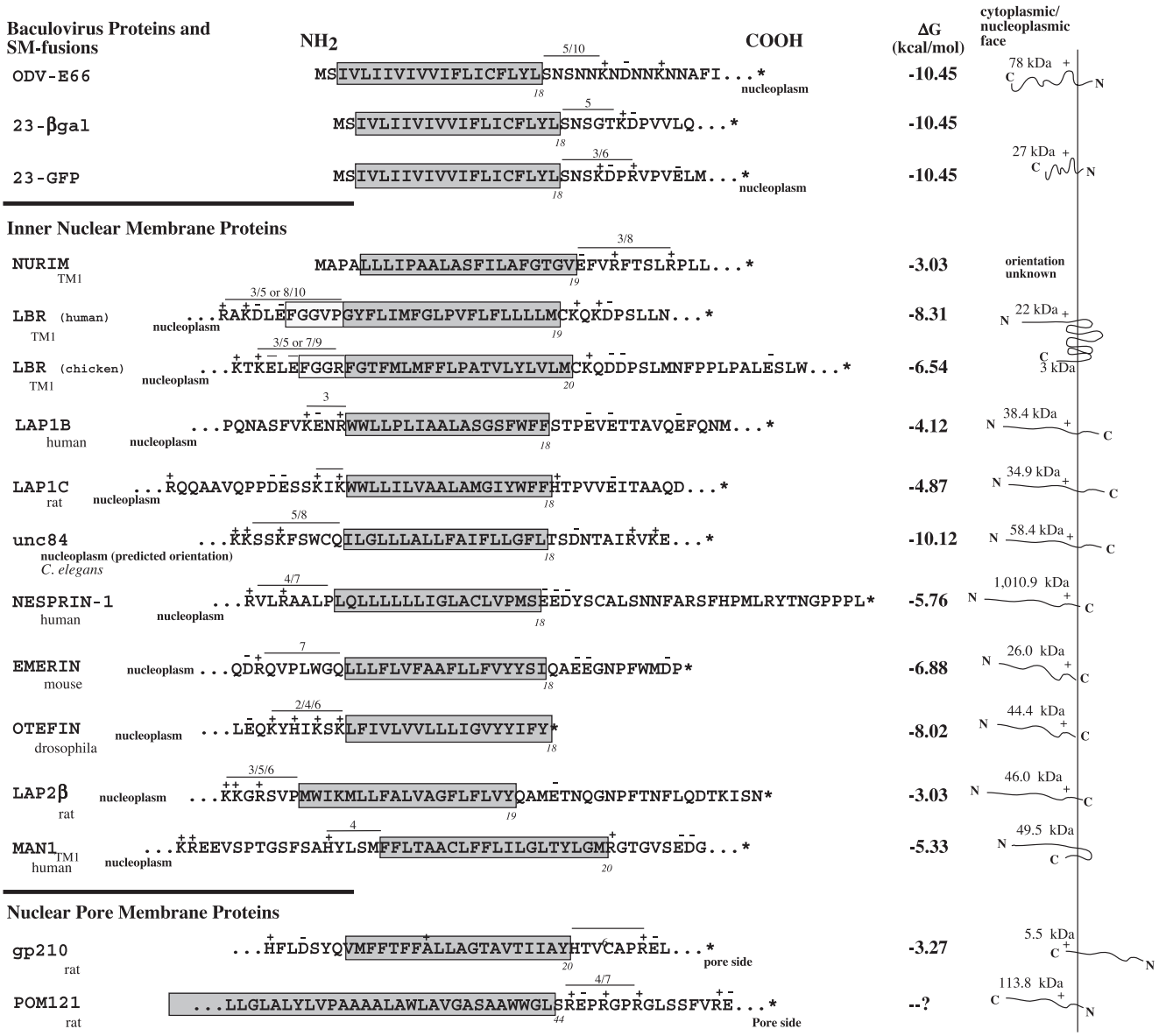

Fig. 5. Comparison of SM with resident INM proteins. (A complete description of this figure and associated references are available in supporting information.) The TM and flanking sequence of the hydrophobic sequence most likely to influence INM localization are shown. The Δ*G* for membrane insertion was calculated by using the White–Wimley (octanol interface) scale. The orientation is shown with placement of the positively charged amino acids on the cytoplasmic/nucleoplasmic face noted.

and E26 precipitate the free SM cassette (Fig. 4*B*, lanes 3 and 5, and 4*C*, lanes 12 and 13), whereas they cannot precipitate the SM cassette in the absence of cross-linking reagent (Fig. 4*B*, lanes 4 and 6). Antibody precipitations were performed by using buffer that should denature protein complexes; thus the ability of the SM cassette to remain associated with either FP25K or E26 suggests the cross-linking reagent is doing something to help maintain association of the noncovalently bound proteins in these complexes. Non-cross-linked FP25K binds to the Talon beads (Fig. 4*B*, lane 9); this interaction can be removed by using 8 M urea, whereas the binding of the cross-linked complex to Talon or Ni^{++} remains (data not shown).

The SM cassette cross-linking with FP25K and/or E26 could be the result of a stable interaction occurring within the virion or represent a trafficking intermediate. To discern which, the SM cassette was translated in the presence of infected Sf9 cell microsomes and then treated with BS^3. Antibodies to T7, FP25K, and E26 precipitated the free cassette and the cross-linked complex (Fig. 4*C*, lanes 11–13). To confirm that the spatial positioning of the SM and FP25K or E26 was not occurring within intact virus, antibodies that would precipitate virus in various stages of maturation were tested: p39, ODV-E25, and polyhedrin (precipitate nucleocapsids, mature virus, and partially occluded virus, respectively). None of the antibodies precipitated the translated SM cassette or cross-linked complex (Fig. 4*C*, lanes 14–16). Finally, when a truncated version of E66 (132 aa) was translated *in vitro* and treated with cross-linking reagent, FP25K and E26 were precipitated with E66 antibody (data not shown). We conclude from these experiments that (*i*) the cross-linked complexes are not a result of protein interaction(s) occurring within the assembled virion and (*ii*) are not a result of interactions occurring within the lysine-free portion of the fusion protein. Rather, FP25K and/or E26 are spatially positioned close to the lysines of the SM, while the protein resides within the ER.

Many Resident Proteins of the INM Contain an SM-Like Sequence. There are significant similarities between trafficking of E66 and SM-fusion proteins with resident INM proteins (for a review of INM protein trafficking see ref. 12). Therefore, we asked whether INM proteins contain features similar to the viral SM. Because some INM proteins are polytopic, the comparison was made with the TM sequence known to influence protein localization (Fig. 5 and references shown in supporting information, which is published on the PNAS web site). Most of the TM sequences are similar in length, ranging from 17 to 19 aa. The calculated ΔG values for membrane insertion (kcal/mol) have values ranging from -10.45 (E66) to less favorable values such as -3.03 (nurim). The length and calculated ΔG values of these proteins are similar to examples of resident ER proteins: ribophorin I and II have TM sequences composed of $\approx$19 aa, with ΔG values of -7.13 and -6.87, respectively. The only characteristic we can discern by using computer-assisted or manual "sequence gazing" is a lack of charged amino acids within the hydrophobic sequences.

Because the spacing and orientation of the positively charged amino acids flanking the viral SM seem to be critical for proper protein targeting, we questioned whether the TM sequences of the INM proteins retained these features. The comparison shows that for all the INM proteins with orientation that is known, the orientation and spacing to the charged amino acids is similar to that of the SM: they are present on the nucleoplasmic face and within 5–8 aa from the end of the TM sequence. This is true even if the TM sequence has been shown to play only a minimal role in INM targeting (LAP2, emerin, MAN1, and POM121). Together, these observations suggest that the most relevant TM domains for INM protein trafficking of well characterized INM proteins share characteristics of the viral SM sequence.

Discussion

The N-terminal 33 aa of E66 are sufficient to traffic fusion proteins to the ODV envelope with an efficiency similar to wild-type protein. If the associated charged amino acids are maintained, this sequence can be shortened to 23 aa (1). We show that in the absence of infection, this sequence is also sufficient to promote protein accumulation at the INM (Fig. 2). This sequence contains two features, a hydrophobic sequence and associated charged amino acids oriented on the cytoplasmic/nucleoplasmic face. The mutational analysis showed that the efficiency of protein accumulation at the INM was decreased when placement to the positively charged lysines was altered (Fig. 3).

If protein–protein interactions are important for viral SM-fusion trafficking, such interactions should be at optimal levels during viral infection. Thus, experiments were designed to identify such interactions using infected cells and the lysines of the SM as bait. Chemical cross-linking experiments resulted in cross-linked complexes containing two viral proteins: FP25K and/or E26. Because FP25K has already been implicated in the trafficking of E66 (7, 13), its identification here poses the possibility that it directly interacts with E66. The function of FP25K and E26 are undetermined; however, it has been speculated that they interact with actin and/or cytoplasmic dynein (14).

The data in this article suggest that once inserted into the ER, the SM fusion interacts with the viral proteins FP25K and/or E26 during trafficking to the nuclear envelope. The possibility that E66 required other viral proteins for efficient passage from the ER to the INM was first postulated when it was observed that E66 accumulated in punctate regions associated with the ONM and was not detected at the INM or to viral-induced membranes within the nucleus when *FP25K* was deleted from the genome (7, 13). These results suggest that FP25K may affect passage of E66 from the ONM to the INM, potentially by facilitating trafficking through the lateral channels of the nuclear pore.

In the absence of infection, SM-fusion proteins are present within the ER; however, they also show a distinct rim at the INM. This is surprising, because E66 or SM fusions do not contain sequences that would predict binding to nucleoplasmic proteins or DNA. Considering that mammalian resident INM proteins also contain features similar to the viral SM, it is possible that the SM-like sequences facilitate accumulation at the INM, and this is independent of retention sequences. Thus, the SM-like sequence may be sufficient to promote directional movement but not immobilization at the INM.

It is known that cytoplasmic intraorganelle movement of membrane proteins is highly regulated and includes protein–protein and protein–lipid interactions. Although it is possible that the continuous membranes of the ER, ONM, pore membrane, and INM require a less elaborate mechanism of trafficking, it is possible also that more than one mechanism exists for ER-to-INM trafficking. The diffusion-retention model (12) may describe the essential features for some resident INM proteins; however, proteins containing larger cytoplasmic domains (e.g., Nesprin-1; Fig. 5) may require other factors for optimal passage across the nuclear pore lateral channels. We propose that the viral protein E66 may be an example of such a protein. E66 exposes most of its mass at the cytoplasmic face; thus during passage across the lateral channels, the exposed protein would be at the upper limit of free passage [$\approx$76 kDa (15)]. Considering trafficking to the INM has been studied in detail for only a few proteins, it remains to be determined whether trafficking for the increasing complement of proteins that compose the INM will be explained successfully by diffusion retention or whether multiple pathways and/or regulatory events function in this pathway.

Microsomal membrane preparations and selected experiments were performed in the laboratory of Art Johnson, whom we thank for unfailing support of this work and for providing the Bcl_2 gene that was incorporated into the sorting-motif cassette. We also thank Yuanlong Shao for making the insect microsomes and Paul Fisher for antibody to *Drosophila* lamin (ADL67). This work was supported by Texas Agricultural Experiment Station Project TEXO-08078 (M.D.S.). This article was submitted by S.T.W. and S.S. in partial fulfillment of the Ph.D. degree at Texas A&M University.

1. Hong, T., Braunagel, S. C. & Summers, M. D. (1997) *Proc. Natl. Acad. Sci. USA* **94,** 4050–4055.
2. Summers, M. D. & Smith, G. E. (1987) *Tex. Agric. Experiment Stn. Bull.*, no. 1555.
3. Liao, S., Lin, J., Do, H. & Johnson, A. E. (1997) *Cell* **90,** 31–41.
4. Walter, P. & Blobel, G. (1983) *Methods Enzymol.* **96,** 84–93.
5. Braunagel, S. C., Elton, D., Ma, H. & Summers, M. D. (1996) *Virology* **217,** 97–110.
6. Adam, S. A., Sterne-Marr, R. & Gerace, L. (1992) *Methods Enzymol.* **219,** 97–110.
7. Rosas-Acosta, G., Braunagel, S. C. & Summers, M. D. (2001) *J. Virol.* **75,** 10829–10842.
8. Stuurman, N., Maus, N. & Fisher, P. A. (1995) *J. Cell Sci.* **108,** 3137–3144.
9. Hong, T., Braunagel, S. C. & Summers, M. D. (1994) *Virology* **204,** 210–222.
10. Jadot, M., Hofmann, M. W., Graf, R., Quader, H. & Martoglio, B. (1995) *FEBS Lett.* **371,** 145–148.
11. Braunagel, S. C., Russell, W. K., Rosas-Acosta, G., Russell, D. H. & Summers, M. D. (2003) *Proc. Natl. Acad. Sci. USA* **100,** 9797–9802.
12. Worman, H. J. & Courvalin, J.-C. (2000) *J. Membr. Biol.* **177,** 1–11.
13. Braunagel, S. C., Burks, J. K, Rosas-Acosta, G., Harrison, R. L., Ma, H. & Summers, M. D. (1999) *J. Virol.* **73,** 8559–8570.
14. Beniya, H., Braunagel, S. C. & Summers, M. D. (1998) *Virology* **240,** 64–75.
15. Hinshaw, J. E., Carragher, B. O. & Milligan, R. A. (1992) *Cell* **73,** 1267–1279.